MRI Sequences and Diagnostic Accuracy in Placenta Accreta Spectrum: A Comparison of T2WI and T2WI+DWI with Surgical and Histopathology Results

Lies Mardiyana[a], Fallis Desita[a], Tri Wulanhandarini[a], Widiana Ferriastuti[a], Grace Ariani[b], Rozi Aryananda[c,d]

Email: falisius@gmail.com

[a]Department of Radiology, Faculty of Medicine, Universitas Airlangga, Dr Soetomo Academic General Hospital, Surabaya Indonesia
[b]Department of Anatomical pathology, Faculty of Medicine, Universitas Airlangga, Dr Soetomo Academic General Hospital, Surabaya Indonesia
[c]Department of Obstetrics & Gynecology, Faculty of Medicine, Universitas Airlangga, Dr Soetomo Academic General Hospital, Surabaya Indonesia
[d]Department of Obstetrics & Gynecology, Erasmus University Medical Center, Rotterdam, The Netherland

Abstract

Objective: This study compares the Magnetic Resonance Imaging (MRI) sequences T2-Weighted Imaging (T2WI) and T2WI+Diffusion-Weighted Imaging (DWI) in the placenta accreta spectrum (PAS) with the findings of surgery and histopathology.
Study Design: We conducted a retrospective cohort study of consecutive prenatally suspected PAS cases in a single tertiary-care PAS center who underwent non-contrast pelvic MRI at our hospital from 2018 to April 2023. The data were analysed to compare the multiplanar T2WI and multiplanar T2WI + DWI axial sections between the International Federation of Gynecology and Obstetrics (FIGO)-modified classification groups of degrees 1-2 and degree 3 (according to the surgical findings) as well as the "accreta-increta" and "percreta" groups (according to the histopathological findings)
Result: There were 35 patients, six women (17.1%) in the FIGO grades 1-2 group and 29 women (82.8%) in the FIGO grade 3 group, according to the surgical findings. In addition, 29 women (82.8%) were included in the "Accreta-Increta" group, and six women (17.1%) were included in the "Percreta" group, according to the histopathological findings. The T2WI sequence showed a significantly higher difference in assessing loss of retroplacental dark zone and bladder wall interruption in the FIGO-modified classification compared to the T2WI+DWI sequence (p=0.026 vs p=0.063; p=0.008 vs p=0.146). In analysing each PAS subtype histopathologically, there were no significant variations in MRI features between the T2WI and T2WI+ DWI sequences.
Conclusion: The addition of axial DWI sequences to multiplanar T2WI MRI sequences did not significantly provide additional information in relation with clinical and histopathology grading of placenta accreta spectrum.

Keywords: T2W; DWI; Diffusion Weighted Imaging; Placenta Accreta Spectrum; PAS

1. Introduction

Placenta Accreta Spectrum (PAS) is one of the most difficult situation for cesarean section in order to its difficult surgery and high morbidity (Nieto-Calvache et al., 2021). It is the leading cause of postpartum haemorrhage with a high fatality rate (Aryananda et al., 2023). Over the previous four decades, the global incidence of placenta accreta has increased from 1:30,000 to 1:300 pregnancies. The incidence is rising with the increase in elective cesarean section deliveries (Kapoor et al., 2021; Morel et al., 2019).

Placenta accreta is usually detected on the lower anterior uterine wall and relates to previous caesarean section surgery. Scar tissue frequently accumulates at the surgical site, along with adhesions in the cervix, bladder wall, and parametrium, neovascularisation, and myometrial tissue damage, making surgical methods for PAS more challenging. Magnetic resonance imaging (MRI) can provide comprehensive topographical and morphological information in areas where ultrasonography (USG) is inefficient (Finazzo et al., 2020; Palacios-Jaraquemada & D'antonio, 2021; Srisajjakul et al., 2021).

The T2 Weighted Imaging (T2WI) sequence is a standard sequence widely used to assess placental attachment and shows the anatomy of the placenta and myometrium. The T2WI sequence has a short duration (about 60-90 seconds) but is impacted by motion artefacts such as breathing and fetal movement. Meanwhile, Diffusion-weighted imaging (DWI) sequence is thought to provide a better view of the placenta-myometrial interface and focal myometrial thinning than T2WI sequence (about 3-4 minutes). Hence, the addition of the DWI sequence to the diagnosis of placenta accreta spectrum is presumed to improve the accuracy of PAS diagnosis (Fornasa & Montemezzi, 2012; Morita et al., 2009).

2. Methode

This is a retrospective cohort study conducted during 18 months (January 2021 till April 2023) in a single tertiary-care PAS center, Dr. Soetomo Academic General Hospital, in Indonesia. All women with a previous cesarean section and a placenta were identified as having risk factors for PAS and screened by ultrasound and the MRI. This study's subject inclusion criteria were as follows: (1) complete MRI pictures (T2WI and DWI sequences); (2) high image quality (no motion artefacts and increased noise); (3) Histopathology reports and appropriate caesarean delivery records. Incomplete data of medical record and pathology result were excluded. The University Institutional Review Board (IRB) for Imaging Research Institute authorized this retrospective investigation.

2.1. MRI Protocol

The patients were fully bladder and supine position utilizing a pelvic phased-array coil on 1.5T and 3T MR machines without using contrast. T2W images were obtained using Half-Fourier Single-shot Turbo Spin Echo (HASTE), which comprises the axial, coronal, and sagittal planes (field of view [FOV] = 350-400, matrix = 320 x 192, repetition time/time to echo [TR/TE] = 1100/97, slice thickness = 4.0 mm, and interslice gap = 1.0). The axial plane of a DWI sequence was acquired with b values of 800 and apparent diffusion coefficient (ADC) maps (FOV = 320-400, TR/TE = 11400/48, slice thickness = 4.0 mm, interslice gap = 1.0).

All MR images were examined by two female consultant radiologists who were blinded to the final diagnosis and had experience interpreting pelvic MRI. The clinical outcomes and pathology were correlated between groups with statistically substantial interrater reliability tests of Cohen's Kappa. A comparative analysis was performed to compare Observer 1 with Observer 2. Kappa values of 0.01-0.20 are viewed as modest, 0.21-0.40 as fair, 0.41-0.60 as moderate, and 0.81-1.00 as very good to virtually perfect. Statistical Package for the Social Sciences (SPSS) software 29.0 IBM Inc. was used for statistical analysis. A value of 0.05 or less is deemed statistically significant. MRI examinations were analyzed for the presence of several findings, including heterogeneous placenta, placental bulge, dark intraplacental bands, loss of retroplacental dark zone, placental ischemic infarction, myometrial thinning, bladder wall interruption, focal exophytic mass, and abnormal vascularisation of the placental bed (Morel et al., 2019).

The FIGO-modified classification criteria were utilized in this study, separated into two groups based on surgical findings: group 1 had FIGO grades 1 and 2, whereas group 2 had FIGO grade 3. Furthermore, the

participants were also separated into two groups based on histological findings. Placenta accreta and increta were included in Group 1, while placenta percreta was included in Group 2. The categorization for the placenta accreta spectrum developed by FIGO is based on intraoperative results and has been updated considering new research (Jauniaux *et al.*, 2022). This categorization is used to diagnose and categorize the severity of PAS. The FIGO classification is divided into the following groups:

- Grade I: There is no placental tissue invading the uterine surface, no visible bulge, no placental tissue infiltrating the uterine surface, and nil or limited neovascularisation.
- Grade II: There is a placental bulge and bluish/purple colouring, hyper-vascularisation along the uterine craniocaudal serosa, no placental tissue invading the uterine surface, and cord traction causes the uterus to be somewhat dragged inward (dimple sign).
- Grade III
  - 3a: The presence of a thinned serosa with the placenta clearly visible, an obvious bulge and neovascularity on the serosa surface; there is no invasion of other organs in the pelvic cavity, and the bladder-uterus boundary can still be seen during surgery.
  - 3b (bladder invasion): Only placental villi invade the bladder; no other organs in the pelvic cavity are invaded, and the boundary between the bladder and uterus is difficult to determine after surgery.
  - 3c (placental tissue invasion of other organs in the pelvic cavity): Placental tissue is visible, penetrating the broad ligament, vaginal wall, pelvic wall, and other organs in the pelvic cavity (with or without bladder invasion).

The degree of placental attachment to the uterus and surrounding organs is related to complications in PAS patients. According to FIGO, grades 1-2 are less severe than grades 3. MRI to detect the degree of PAS attachment is intended to aid in determining appropriate treatment, which may differ between PAS grades 1-2 and grade 3 during delivery. Criteria for histopathological diagnosis according to the adherent of chorionic villi to the myometrium (accreta – only attach on myometrium; increta – invade the myometrium; percreta – penetrate the uterine serosa and occasionally attach other pelvic organs) (Bourgioti *et al.*, 2018; Hecht *et al.*, 2020).

3. Results

Fifty-one women had MRI during this period and 35 women were included in this study after inclusion and exclusion were applied. Based on surgical result, six women were classified as FIGO grades 1-2 which is less severe condition, while twenty nine women were classified as FIGO grade 3, refers to the most severe condition . According to histopathological findings, 29 women were assigned to the "Accreta-Increta" group, and 6 were assigned to the "Percreta" group. There were 24 persons (68.6%) over the age of 35, and 11 people (31.6%) were over the age of 35. Furthermore, two people (5.7%) had no prior caesarean section surgery history, 12 people (24.3%) had one caesarean section surgery history, and 21 people (60%) had two caesarean section procedures. Placenta previa was identified in all cases of the placenta accreta spectrum.

The presence of descriptors related to FIGO grades are reported in table 1 and 2. There are only two significant predictors on the T2WI sequences, however there was no significant difference in T2WI+DWI sequences. The loss of the retroplacental dark zone had a greater severity risk after multivariate analysis in T2WI sequences. Some of MRI characteristics cannot be assessed because they are constant and present in all MRI examinations, both in surgical and histopathological findings. Moreover, the MRI parameters of T2WI

and T2WI+DWI in histopathological results did not differ significantly between the accreta-increta and percreta groups (table 3).

Table 1. T2WI Sequence Magnetic Resonance Imaging Signs Related To FIGO Modified Classification Of Placenta Accreta Spectrum

	Grade 1 – 2 (n=6)	Grade 3 (n=29)	p-value	OR (CI 95%)	Sensitivity	Spesificity	PPV	NPV
Heterogenous placenta	6 (100%)	29 (100%)	n/a	n/a				
Placenta bulge	6 (100%)	29 (100%)	n/a	n/a				
Dark intraplacental bands	6 (100%)	29 (100%)	n/a	n/a				
Loss of retroplacental dark zone	3 (50%)	27 (93,1%)	0,026	13,50 (1,57 – 115,93)	93,1	50	90	60
Placental ischemic infarction	0 (0%)	3 (10,3%)	1	-				
Myometrial thinning	4 (66,7%)	27 (93,7%)	0,128	-				
Bladder wall interruption	0 (0%)	18 (62,1%)	0,008	0	62,1	100	100	35,3
Focal exophytic mass	0 (0%)	14 (48,3%)	0,061	-				
Abnormal vascularisation of the placental bed	6 (100%)	29 (100%)	n/a	n/a				
Pathology Result								
Accreta-increta	6	23	0,221	-				
Percreta	0	6						
Vascular sector								
S1	3 (50%)	8 (27,6%)	0,352	-				
S2	3 (50%)	21 (72,4%)						

MRI, Magnetic Resonance Imaging; T2WI, T2-weighted Imaging
FIGO, International Federation of Gynaecology and Obstetrics

Table 2. T2WI+DWI Sequence Magnetic Resonance Imaging Signs Related To FIGO Modified Classification Of Placenta Accreta Spectrum

	Grade 1 – 2 (n=6)	Grade 3 (n=29)	P-value	OR (CI 95%)
Heterogenous placenta	6 (100%)	29 (100%)	N/a	N/a
Placenta bulge	6 (100%)	29 (100%)	N/a	N/a
Dark intraplacental bands	6 (100%)	29 (100%)	N/a	N/a
Loss of retroplacental dark zone	2 (33,3%)	22 (75,9%)	0,063	-
Placental ischemic infarction	0 (0%)	2 (6,9%)	1	-
Myometrial thinning	6 (100%)	27 (93,1%)	1	-
Bladder wall interruption	0 (0%)	11 (37,9%)	0,146	-
Focal exophytic mass	0 (0%)	11 (37,9%)	0,146	-
Abnormal vascularisation of the placental bed	6 (100%)	29 (100%)	N/a	N/a
Vascular sector				
S1	3 (50%)	8 (27,6%)	0,352	-
S2	3 (50%)	21 (72,4%)		
Pathology Result				
Accreta-increta	6	23	0,221	-
Percreta	0	6		

DWI, Diffusion-Weighted Imaging; MRI, Magnetic Resonance Imaging; T2WI, T2-weighted Imaging
FIGO, International Federation of Gynaecology and Obstetrics

The comparison test of categorical agreement between our observers in the T2WI sequence had kappa value of 0.908, while kappa value in T2WI+DWI sequence was 0.898. There were no significant differences in agreement between the T2W only and T2W + DWI reads (p<0,001).

Table 3. T2WI and T2WI+DWI Sequence Magnetic Resonance Imaging Signs Related To Histopathology Results Of Placenta Accreta Spectrum

	T2WI Sequence			T2WI+DWI Sequences		
	Accreta-increta (n=29)	Percreta (n=6)	p-value	Accreta-increta (n=29)	Percreta (n=6)	p-value
Heterogenous placenta	6 (100%)	29 (100%)	N/a	29 (100%)	6 (100%)	N/a
Placenta bulge	6 (100%)	29 (100%)	N/a	29 (100%)	6 (100%)	N/a
Dark intraplacental bands	6 (100%)	29 (100%)	N/a	29 (100%)	6 (100%)	N/a
Loss of retroplacental dark zone	2 (33,3%)	22 (75,9%)	0,063	24 (82,8%)	6 (100%)	0,063
Placental ischemic infarction	0 (0%)	2 (6,9%)	1	3 (10,3%)	0 (0%)	1
Myometrial thinning	6 (100%)	27 (93,1%)	1	25 (86,2%)	6 (100%)	1
Bladder wall interruption	0 (0%)	11 (37,9%)	0,146	15 (51,7%)	3 (50%)	0,146
Focal exophytic mass	0 (0%)	11 (37,9%)	0,146	11 (37,9%)	4 (66,7%)	0,146
Abnormal vascularisation of the placental bed	6 (100%)	29 (100%)	N/a	29 (100%)	6 (100%)	N/a

DWI, Diffusion-Weighted Imaging; MRI, Magnetic Resonance Imaging; T2WI, T2-weighted Imaging

4. Discussion

4.1. Principal Finding

The choice of MRI sequences is critical in identifying placenta accreta diagnosis. MRI can detect the placental position and potential invasive placentation, which is not apparent on ultrasound. This study suggests that DWI mode as additional MRI sequence will not help distinguish the clinical uteroplacental interface. Normal myometrium has three layers (trilaminar) consisting of the uterine serosa in the outermost layer, myometrium in the middle layer, and decidua basalis in the innermost layer, forming the placental-myometrial interface. The retroplacental-myometrial interface appears as a clear space on ultrasound and a hypointense signal on the T2WI sequence. This hypointense signal is known as the retroplacental dark zone. Uterine defects resulting from previous surgery, with an abnormal placental adherent to the uterine serosa cause the loss of hypointense signal in this retroplacental area or loss of retroplacental dark zone (Derman *et al.*, 2011; Srisajjakul, Prapaisilp and Bangchokdee, 2021). Bladder wall interruption in MRI have high specificity for high grade of PAS, this signs represent the hypervascularity of uteroplacental interface which is

often seen in high grade PAS (Cali *et al.*, 2017).

4.2. Results in the context of what is known

The loss of the retroplacental dark band and bladder wall interruption were substantially more common on T2WI sequences, warranted in instances with high grade of PAS. Nevertheless, the addition of the DWI sequence as an addition to the T2WI sequence does not provide any evidence of a high grade of PAS (Figures 1 and 2).

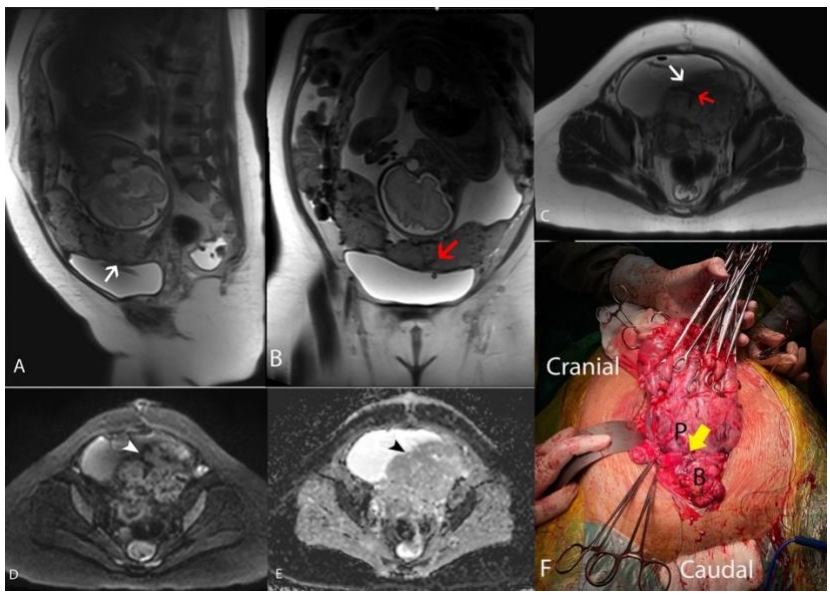

Figure 1. A 36-year-old woman who is 33 weeks pregnant and suspected of having PAS. Pelvic MRI T2WI sequence sagittal (a), coronal (b), and axial (c) sections show bladder wall interuption (white arrow), followed by dark intraplacental bands (red arrow). Axial sections of the DWI sequence (d) and ADC (e) demonstrate non-restricted diffusion at the placental myometrial interface (white head arrow and black head arrow). During surgery, bulging placenta (P) was found on the anterior corpus with bladder attachment (yellow arrow) according to Placenta accreta spectrum FIGO grade 3b. The anatomical pathology results confirmed placenta increta

Sannananja et al. compared PAS and non-PAS cases without grading of PAS. The T2WI sequence exclusively showed that the loss of retroplacental dark zone was more commonly observed in histopathological findings of PAS than non-PAS cases, and it was easier to detect this feature compared to T2WI+DWI sequences (p=0.021 vs p=0.064). In another study, the loss of retroplacental dark zone did not show a significant difference in FIGO grades 1-2 and 3 (p=0.311), nor in accreta-increta and percreta histopathology (p=0.069). According to Morel et al., the presence of bladder wall interruption on MRI could not distinguish between PAS FIGO grades 1-2 and 3 (9.1% vs 24.5%, p=0.11). However, the study only used the T2WI sequence and did not use the DWI sequence (Sannananja *et al.*, 2018; Morel *et al.*, 2021; Pain *et al.*, 2022).

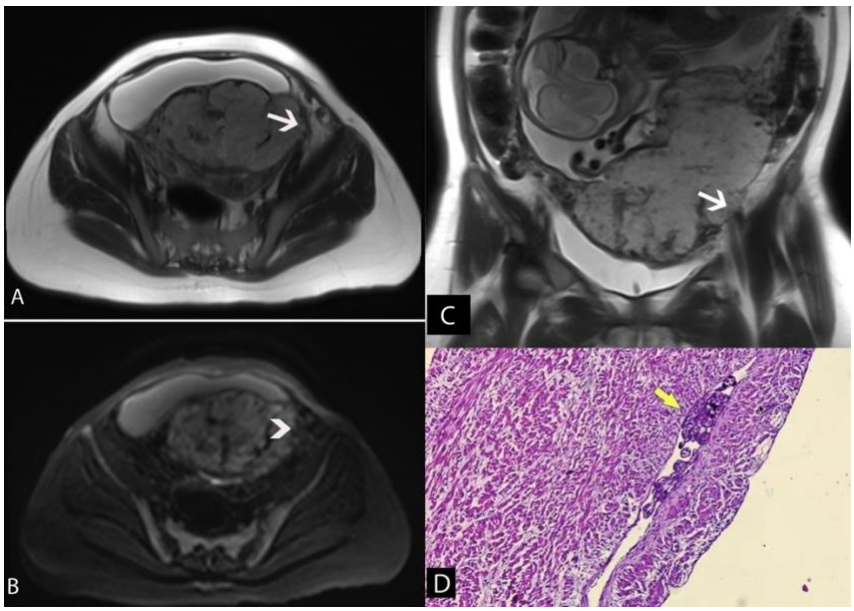

Figure 2. 30-week-pregnant woman with placenta previa and a history of two section cesarean surgery. T2W images axial plane (a) demonstrate that loss of retroplacental dark zone in the left parametrium (white arrow). DWI b = 800 image (b) have low resolution, making it impossible to assess the loss of the retroplacental dark zone sign (white head arrow). T2W images coronal plane (c) confirm the loss of retroplacental dark zone in the left parametrium (white arrow). During the procedure, attachment was found in the left parametrium area. Pathological examination with hematoxylin eosin staining at 100x magnification revealed villi chorealis infiltrate the myometrium (yellow arrow) (d)

4.3. Clinical Implications

The common topography of PAS is mainly above bladder trigone in relation with previous caesarean section location (Palacios-Jaraquemada *et al.*, 2022). However, different types of PAS topography—such as the parametrium, posterior, and lower bladder trigone—present particular difficulties. Lower topography has a greater risk of massive blood loss during surgery in comparison to upper topography, despite being less common. The massive blood loss may relate to the pelvic anastomosis to the uteroplacental angiogenesis and remodeling (Alessandrini *et al.*, 2023). MRI can show topography well which identifying loss of retroplacental dark zone and bladder wall interruption may represent lower topography with high grade of PAS. This may be useful information during surgery and help the surgeon to preparing such as blood transfusion, possibility for uterine conservative surgery, or aortic control to reduce the blood loss. Additionally, remodeling induces significant morphological alterations in the lower segment of the uterus, such as focal myometrial thinning and pseudo bulging evident on ultrasound, MRI, and upon delivery, yet histological investigation reveals no chorionic villi in the area – this may explain why the addition of DWI sequences is difficult to distinguish between actual placental bulging caused by the placental invasion and pseudo bulging caused by the remodeling process (figure 3) (Jauniaux *et al.*, 2022).

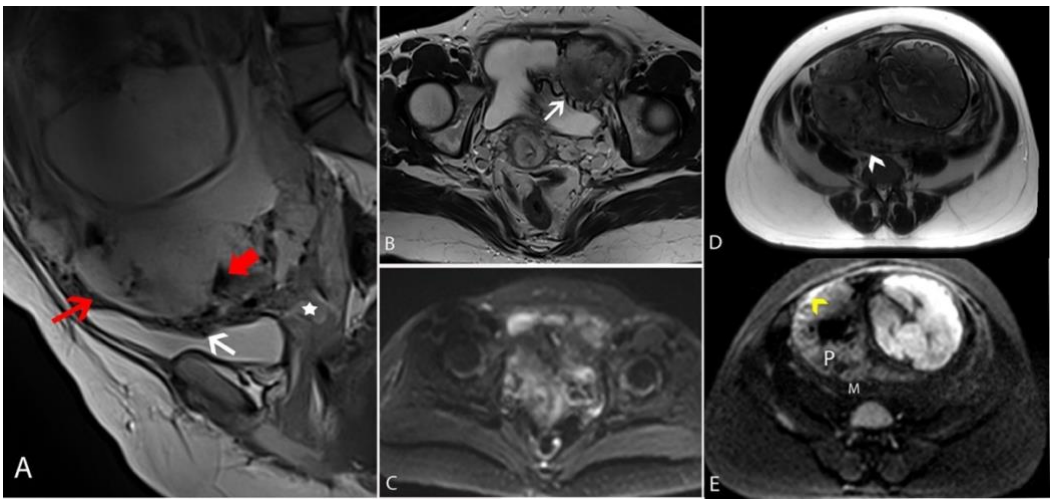

Figure 3. T2WI sequence (a) sagittal and (b) axial plane show placental bulge (thin red arrow) dan placental heterogeneity with dark intraplacental bands (thick red arrow) and hypervascularity (thin white arrow in a and b). There is also placenta previa total with unclear borders on the cervix suggest cervical adherent (white star). DWI sequence (c) axial plane shows an image with low resolution, making vascularization difficult to identify. T2WI sequence (d) axial plane shows unclear boundaries between the placental-myometrial interface (white head arrow), while the DWI sequence (e) shows a hyperintense placental (P) area with thinning myometrium (M), especially on the anterior side (yellow head arrow)

Most cases of placenta percreta will have a partial or whole uterine rupture, dehiscence, and adhesions, particularly in the anterior lower segment and posterior bladder wall. In Bourgioti et al.'s study, more than half of the PAS patients had bladder invasion, and several required significant bladder wall repair or partial cystectomy. Unlike cancer cases, this placental tissue adheres tightly to the bladder wall and induces new vascularisation rather than penetrating the bladder wall. The findings of intraoperative cystoscopy demonstrate changes in the posterior bladder mucosa without placental tissue penetrating the bladder. Moreover, the tied placental tissue is highly fragile and frequently results in significant haemorrhage. According to Jariyawattanarat et al., abnormal bladder attachment in PAS relates to severe haemorrhage during delivery (p=0.022). Another study found that bladder attachment had no significance on the histological diagnosis of placenta percreta since the placental tissue that adheres to the bladder is left behind and not removed during surgery; therefore, the histopathological examination was not mainly performed on the area that experiences adhesion (Bourgioti *et al.*, 2018; Jauniaux, Collins and Burton, 2018; Knight *et al.*, 2018; Jauniaux *et al.*, 2022; Jariyawattanarat *et al.*, 2023).

4.4. Research Implications

On both T2WI and T2WI+DWI sequences, the general characteristics of MRI did not demonstrate a significant difference in distinguishing placenta accreta-increta and percreta histopathologically. The majority of the samples in this investigation were scanned with T2 HASTE in MRI. According to Kim et al.'s investigation, the T2 True fast imaging with steady-state precession (FISP) (Balanced gradient echo) and HASTE (Ultrafast spin echo) sequences are effective in detecting placenta accreta. This approach generates higher-quality photos in less time, explaining why DWI sequences did not provide new information for diagnosing PAS in this study (Kim and Narra, 2004; Tamai *et al.*, 2007). Loss of retroplacental dark zone is best seen on T2WI sequences.

4.5. Strengths and Limitations

One of the limitations of DWI sequences is that they cannot detect placenta accreta due to a decidua layer defect without focal thinning or abnormal myometrial attachment. Furthermore, DWI sequences have lower resolution than T2WI sequences in measuring the loss of the retroplacental dark zone – this could explain why T2WI sequence interpretation is superior to DWI sequence interpretation (Sannananja *et al.*, 2018; Jha *et al.*, 2020; Morel *et al.*, 2021). Besides, T2WI sequences are used to assess bladder adherence in PAS by analysing the hypointensity signal of the bladder serosa and are best evaluated on sagittal slices. T2WI sequences were more significant in identifying the severity of PAS according to FIGO in this investigation than T2WI+DWI sequences. T2WI sequences were multiplanar (axial, coronal, and sagittal), whereas DWI sequences were only axial. Furthermore, the axial section in DWI sequences may cause partial volume impact, resulting in a less accurate diagnosis (Sannananja *et al.*, 2018; Zawaideh *et al.*, 2022; Patel-Lippmann *et al.*, 2023). Because there was no control group (placenta previa only without PAS) in this study, the MRI parameters cannot be utilised to assess the strength and accuracy of PAS diagnosis in general. The MRI parameters evaluated were more concerned with determining the extent of placental invasion using FIGO and histopathology. There are only a few studies comparing MRI sequences for PAS diagnosis, making comparisons challenging.

5. Conclusion

Integrating axial DWI sequences into multiplanar T2WI MRI sequences did not provide significant extra information that could help in MRI screening of placenta accreta spectrum, particularly in relation with clinical and histopathological grading. Although the MRI may help in distinguish the placental topography which related with surgical dificulties.

Acknowledgements

I would like to express my gratitude to all staff in Department of Radiology, Department of Anatomical pathology dan also Department of Obstetrics & Gynecology, Dr. Soetomo Academic General Hospital, for their unwavering support and guidance throughout the course of my research. Their expertise and insights have provided valuable perspectives and have contributed to the overall excellence of this research.

References

Alessandrini, L. *et al.* (2023) 'The correlation between serum levels and placental tissue expression of PLGF and sFLT-1 and the FIGO grading of the placenta accreta spectrum disorders', *The Journal of Maternal-Fetal & Neonatal Medicine*, 36(1). Available at: https://doi.org/10.1080/14767058.2023.2183744.

Aryananda, R.A. *et al.* (2023) 'Management of unexpected placenta accreta spectrum cases in resource-poor settings', *AJOG Global Reports*, 3(2), p. 100191. Available at:

https://doi.org/https://doi.org/10.1016/j.xagr.2023.100191.

Bourgioti, C. *et al.* (2018) 'MRI features predictive of invasive placenta with extrauterine spread in high-risk gravid patients: A prospective evaluation', *American Journal of Roentgenology*, 211(3), pp. 701–711. Available at: https://doi.org/10.2214/AJR.17.19303.

Cali, G. *et al.* (2017) 'Ultrasound Detection of Bladder-Uterovaginal Anastomoses in Morbidly Adherent Placenta.', *Fetal diagnosis and therapy*, 41(3), pp. 239–240. Available at: https://doi.org/10.1159/000445055.

Derman, A.Y. *et al.* (2011) 'MRI of placenta accreta: A new imaging perspective', *American Journal of Roentgenology*, 197(6), pp. 1514–1521. Available at: https://doi.org/10.2214/AJR.10.5443.

Finazzo, F. *et al.* (2020) 'Interobserver agreement in MRI assessment of severity of placenta accreta spectrum disorders', *Ultrasound in Obstetrics and Gynecology*, 55(4), pp. 467–473. Available at: https://doi.org/10.1002/uog.20381.

Fornasa, F. and Montemezzi, S. (2012) 'Diffusion-weighted magnetic resonance imaging of the normal endometrium: Temporal and spatial variations of the apparent diffusion coefficient', *Acta Radiologica*, 53(5), pp. 586–590. Available at: https://doi.org/10.1258/ar.2012.110717.

Hecht, J.L. *et al.* (2020) 'Classification and reporting guidelines for the pathology diagnosis of placenta accreta spectrum (PAS) disorders: recommendations from an expert panel', *Modern Pathology*, 33(12), pp. 2382–2396. Available at: https://doi.org/10.1038/s41379-020-0569-1.

Jariyawattanarat, W. *et al.* (2023) 'Bladder involvement in placenta accreta spectrum disorder with placenta previa: MRI findings and outcomes correlation', *European Journal of Radiology*, 160. Available at: https://doi.org/10.1016/j.ejrad.2023.110695.

Jauniaux, E. *et al.* (2022) 'Searching for placenta percreta: a prospective cohort and systematic review of case reports', *American Journal of Obstetrics and Gynecology*, 226(6), pp. 837.e1-837.e13. Available at: https://doi.org/10.1016/j.ajog.2021.12.030.

Jauniaux, E., Collins, S. and Burton, G.J. (2018) 'Placenta accreta spectrum: pathophysiology and evidence-based anatomy for prenatal ultrasound imaging', *American Journal of Obstetrics and Gynecology*. Mosby Inc., pp. 75–87. Available at: https://doi.org/10.1016/j.ajog.2017.05.067.

Jha, P. *et al.* (2020) 'Nonfetal Imaging During Pregnancy: Placental Disease', *Radiologic Clinics of North America*. W.B. Saunders, pp. 381–399. Available at: https://doi.org/10.1016/j.rcl.2019.11.004.

Kapoor, H. *et al.* (2021) 'Review of MRI imaging for placenta accreta spectrum: Pathophysiologic insights, imaging signs, and recent developments', *Placenta*. W.B. Saunders Ltd, pp. 31–39. Available at: https://doi.org/10.1016/j.placenta.2020.11.004.

Kim, J.A. and Narra, V.R. (2004) 'Magnetic resonance imaging with true fast imaging with steady-state precession and half-Fourier acquisition single-shot turbo spin-echo sequences in cases of suspected placenta accreta', *Acta Radiologica*, 45(6), pp. 692–698. Available at: https://doi.org/10.1080/02841850410001114.

Knight, J.C. *et al.* (2018) 'A comprehensive severity score for the morbidly adherent placenta: combining ultrasound and magnetic resonance imaging', *Pediatric Radiology*, 48(13), pp. 1945–1954. Available at: https://doi.org/10.1007/s00247-018-4235-4.

Morel, O. *et al.* (2019) 'A proposal for standardized magnetic resonance imaging (MRI) descriptors of abnormally invasive placenta (AIP) – From the International Society for AIP', *Diagnostic and Interventional Imaging*, 100(6), pp. 319–325. Available at: https://doi.org/10.1016/j.diii.2019.02.004.

Morel, O. *et al.* (2021) 'Performance of antenatal imaging to predict placenta accreta spectrum degree of severity', *Acta Obstetricia et Gynecologica Scandinavica*, 100(S1), pp. 21–28. Available at: https://doi.org/10.1111/aogs.14112.

Morita, S. *et al.* (2009) 'Feasibility of diffusion-weighted MRI for defining placental invasion', *Journal of Magnetic Resonance Imaging*, 30(3), pp. 666–671. Available at: https://doi.org/10.1002/jmri.21875.

Nieto-Calvache, A.J. *et al.* (2021) 'Lack of experience is a main cause of maternal death in placenta accreta

spectrum patients', *Acta Obstetricia et Gynecologica Scandinavica*, 100(8), pp. 1445–1453. Available at: https://doi.org/https://doi.org/10.1111/aogs.14163.

Pain, F.A. *et al.* (2022) 'Percreta score to differentiate between placenta accreta and placenta percreta with ultrasound and MR imaging', *Acta Obstetricia et Gynecologica Scandinavica*, 101(10), pp. 1135–1145. Available at: https://doi.org/10.1111/aogs.14420.

Palacios-Jaraquemada, J.M. *et al.* (2022) 'Placenta accreta spectrum: a hysterectomy can be prevented in almost 80% of cases using a resective-reconstructive technique', *The Journal of Maternal-Fetal & Neonatal Medicine*, 35(2), pp. 275–282. Available at: https://doi.org/10.1080/14767058.2020.1716715.

Palacios-Jaraquemada, J.M. and D'antonio, F. (2021) 'Posterior placenta accreta spectrum disorders: Risk factors, diagnostic accuracy, and surgical management', *Maternal-Fetal Medicine*. Wolters Kluwer Health, pp. 268–273. Available at: https://doi.org/10.1097/FM9.0000000000000124.

Patel-Lippmann, K.K. *et al.* (2023) 'Placenta Accreta Spectrum Disorders: Update and Pictorial Review of the SAR-ESUR Joint Consensus Statement for MRI', *Radiographics : a review publication of the Radiological Society of North America, Inc*, 43(5), p. e220090. Available at: https://doi.org/10.1148/rg.220090.

Sannananja, B. *et al.* (2018) 'Utility of diffusion-weighted MR imaging in the diagnosis of placenta accreta spectrum abnormality', *Abdominal Radiology*, 43(11), pp. 3147–3156. Available at: https://doi.org/10.1007/s00261-018-1599-8.

Srisajjakul, S., Prapaisilp, P. and Bangchokdee, S. (2021) 'Magnetic Resonance Imaging of Placenta Accreta Spectrum: A Step-by-Step Approach', *Korean journal of radiology*. NLM (Medline), pp. 198–212. Available at: https://doi.org/10.3348/kjr.2020.0580.

Tamai, K. *et al.* (2007) 'Diffusion-weighted MR imaging of uterine endometrial cancer', *Journal of Magnetic Resonance Imaging*, 26(3), pp. 682–687. Available at: https://doi.org/10.1002/jmri.20997.

Zawaideh, J.P. *et al.* (2022) 'Placental MRI: Identification of radiological features to predict placental attachment disease regardless of reader expertise', *European Journal of Radiology*, 149. Available at: https://doi.org/10.1016/j.ejrad.2022.110203.